Journal of Crystal Growth 511 (2019) 56–60

Contents lists available at ScienceDirect

Journal of Crystal Growth

journal homepage: www.elsevier.com/locate/jcrysgro

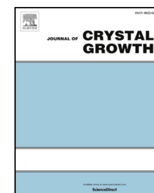

O-band InAs/GaAs quantum dot laser monolithically integrated on exact (0 0 1) Si substrate

Keshuang Li[a], Zizhuo Liu[a], Mingchu Tang[a,⁎], Mengya Liao[a], Dongyoung Kim[a], Huiwen Deng[a], Ana M. Sanchez[b], R. Beanland[b], Mickael Martin[c], Thierry Baron[c], Siming Chen[a], Jiang Wu[a], Alwyn Seeds[a], Huiyun Liu[a]

[a] Department of Electronic and Electrical Engineering, University College London, London WC1E 7JE, United Kingdom
[b] Department of Physics, University of Warwick, Coventry CV4 7AL, United Kingdom
[c] Univ. Grenoble Alpes, CNRS, CEA-LETI, MINATEC, LTM, F-38054 Grenoble, France

ARTICLE INFO

Keywords:
A1. Low dimensional structures
A3. Molecular beam epitaxy
B2. Semiconducting III-V materials
B3. Laser Diodes

ABSTRACT

The concept of high-efficiency, high-reliability and low-threshold electrically pumped lasers monolithically grown on silicon has attracted great attention over the past several decades, as a promising on-chip optical source for Si photonics. In this paper, we report an electrically pumped continuous-wave (CW) 1.3 µm InAs/GaAs quantum dot (QD) lasers grown on a complementary metal-oxidesemiconductor (CMOS) compatible Si exact (0 0 1) substrate with reduced GaAs buffer thickness down to ~2 µm. A threshold current density (J_{th}) as low as ~160 A/cm^2 has been achieved at room temperature. The characteristic temperature (T_0) obtained is ~60.8 K and laser operation is observed up to 52 °C under CW mode. These results suggest that an O-band InAs/GaAs QD laser could be very promising to develop a monolithically integrated on-chip optical source for Si photonics.

1. Introduction

Rapidly growing data traffic has led to extensive research interest on Si based photonic integrated circuits for use in data centers due to the potential to improve dramatically the data rate, integration density, fabrication cost, and power dissipation, comparing with the copper interconnection [1,2]. As a crucial component, the lack of a reliable Si based on-chip optical source has limited the commercialization of Si based photonic integrated circuits [3–5]. Although impressive breakthroughs for group IV laser have been achieved in recent years [6–8], integrating III-V lasers on Si remains the preferred solution because of their superior optical and electrical properties. In addition, it is expected that III-V QD lasers integrated on Si will offer high reliability, low threshold current density, and insensitivity to defects and temperature, which makes the integration of III-V QD laser on Si an attractive option for an on-chip light-source on Si [9–11]. It has been proved that stable lasing operation at over 100 °C can be achieved with QD lasers grown on Si [10]. Moreover, for III-V laser grown on Si, QD lasers have shown much higher reliability than corresponding quantum well laser devices [11]. Wafer-bonding and flip-chip bonding techniques for integrating III-V lasers on Si substrate have been successfully demonstrated in the past two decades [12–14]. However, in view of its potential to be a low-cost and high-yield technique, the monolithic integration technique on large scale and complex photonic integrated circuits has drawn much attention in recent years [15].

For the monolithic integration of III-V lasers on Si substrates, large material dissimilarities between III-V and group IV materials in lattice constants, thermal expansion coefficients, and polarities may cause threading dislocations (TDs), micro cracks, and antiphase boundaries (APBs), respectively. All these defects will dramatically degrade the material quality and have negative effects on the laser device performances [16,17]. Several approaches have been utilized to solve these problems. Using InGaAs/GaAs and InAlAs/GaAs strained-layer superlattices (SLSs) as dislocation filter layers (DFLs) has been shown to be effective in suppressing the propagation of TDs, leading to a low threading dislocation density (TDD) of ~10^6/cm^2 for III-V buffer on Si [18]. Reduced buffer thickness not only enhances the coupling efficiency of the grown III-V laser to Si waveguide in silicon-on-insulator (SOI), but also decreases the density of thermal cracks due to the lower total thickness [19]. In order to annihilate APBs, offcut Si substrates have been used to prevent the formation of APBs [11]. Following the report of high performance 1.3 µm electrically pumped InAs/GaAs QD laser on a 4° offcut Si substrate by Wang et al. [20], extensive studies have been devoted to QD lasers on an offcut Si substrate [21–24]. To

⁎ Corresponding author.
E-mail address: mingchu.tang.11@ucl.ac.uk (M. Tang).

https://doi.org/10.1016/j.jcrysgro.2019.01.016

Available online 18 January 2019
0022-0248/ © 2019 The Authors. Published by Elsevier B.V. This is an open access article under the CC BY license (http://creativecommons.org/licenses/BY/4.0/).

date, we have demonstrated a high-performance, high-reliability InAs/GaAs QD laser on offcut Si platform with a low J_{th} ~ 62.5 A/cm^2 and an extrapolated time-to-failure of over 100,158 h [25]. However, as offcut Si substrates are not fully compatible with industrial standard fabrication, realizing a high performance QD laser on an industrial standard CMOS-compatible exact (0 0 1) Si substrate with APB-free buffer is a high priority. So far, notable progresses in InAs/GaAs QD lasers on exact (0 0 1) Si substrates by various approaches has been made [26–31]. We have previously reported the first electrically pumped CW InAs/GaAs QD laser directly grown on an exact GaAs/Si (0 0 1) substrate with a J_{th} of ~425 A/cm^2 with III-As buffer only [26]. High-performance III-V QD lasers on Si (0 0 1) using metal-organic chemical vapor deposition in conjunction with molecular beam epitaxy (MBE) have been demonstrated using V-grooved Si patterned substrates or commercialized exact (0 0 1) GaP/Si substrates, [27–30]. Moreover, pulsed operation from an all-MBE grown InAs QD laser on exact (0 0 1) Si, using an $Al_{0.3}Ga_{0.7}As$ seed layer has been reported by J. Kwoen et al. [31] with J_{th} of ~350 A/cm^2. In this paper, we demonstrate an electrically pumped CW 1.3 µm InAs/GaAs QD laser on a GaAs/Si (0 0 1) substrate using a III-As only buffer layer, enabling J_{th} as low as ~160 A/cm^2 to be achieved.

2. Experiments

2.1. Crystal epitaxial growth

In this work, the InAs/GaAs QD laser structure was epitaxially grown on the GaAs/Si (0 0 1) substrate as shown in Fig. 1. The growth conditions for the buffer have been optimized to reduce the thickness and improve the quality, which is realized on a 300 mm diameter CMOS-compatible on-axis Si (0 0 1) substrate. A two-step 400 nm GaAs layer was grown on the substrate by metal-organic chemical vapor deposition after pre-growth deoxidization. First, a 40 nm low temperature grown GaAs layer (400–500 °C) was deposited as a nucleation layer, then another 360 nm GaAs buffer layer was deposited at relative higher temperature (600–700 °C) [32]. After that, the grown wafer was transferred to the GEN-930 solid-source MBE chamber for the subsequent laser structure growth after dicing to a 2-inch wafer. A 300 nm N-type GaAs buffer layer was initially deposited on the GaAs/Si (0 0 1) substrate to create a smooth surface. Following this, five repeats of N-type 10 nm $In_{0.18}Ga_{0.82}As$/10 nm GaAs SLSs together with a highly doped N-type 300 nm GaAs spacing layer were introduced as one set of DFL to annihilate the TDs. In-situ thermal annealing steps were

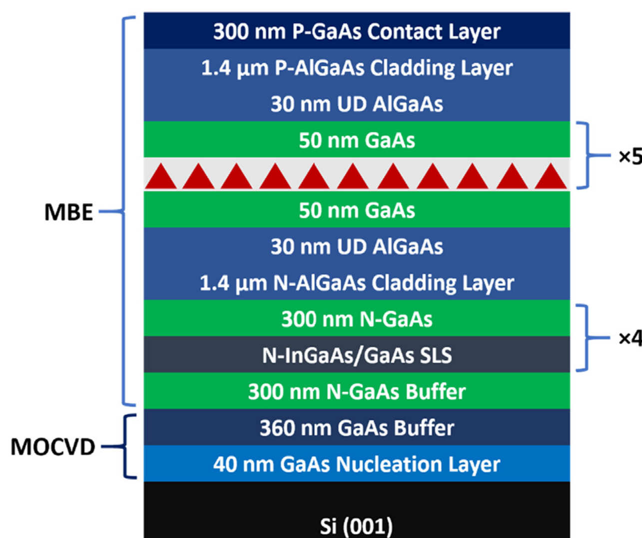

Fig. 1. Schematic structure of InAs/GaAs QD laser directly epitaxy on GaAs/Si (0 0 1) substrate.

performed for each repeat of the SLS in As-rich conditions to help further the TD annihilation [33]. The DFL was repeated for four times to finish the whole buffer growth. Most of the TDs were blocked before the last repeat of $In_{0.18}Ga_{0.82}As$/GaAs SLSs. No extra contact layer was required, since the last set of 300 nm highly doped N-type GaAs was used for the N-contact layer. The reduced total III-V buffer layer thickness is ~2 µm on the exact Si (0 0 1) substrate. Above the DFLs, a 1.4 µm N-type $Al_{0.4}Ga_{0.6}As$ lower cladding layer was deposited. Five layers of InAs/GaAs dot-in-well (DWELL) structure separated by 50 nm GaAs spacer layers formed the active region, which was sandwiched between lower and upper 30 nm undoped AlGaAs guiding layers. Above that, a 1.4 µm P-type $Al_{0.4}Ga_{0.6}As$ upper cladding layer was grown, with a 300 nm highly doped P-type GaAs contact layer at the top of laser structure.

2.2. Measurements

Surface morphologies of the GaAs buffer layer and the InAs/GaAs QDs on Si were characterized by atomic force microscope (AFM) in standard tapping mode in air. Room temperature photoluminescence (PL) and temperature-dependent PL measurements for QDs were performed to study the optical properties. Transmission electron microscopy (TEM) was used to evaluate the movement of TDs and investigate the details of active region. Lasing oscillation with a low J_{th} was achieved at room temperature in CW mode.

Fig. 2(a) shows a 5 µm × 5 µm AFM image of a 400 nm GaAs buffer layer by two-step growth on exact Si (0 0 1) substrate. It can be seen that the surface is APB-free and flat with small root mean square (RMS) surface roughness of 0.81 nm. Fig. 2(b) shows a typical 1 µm × 1 µm AFM image of uncapped QDs grown under the same conditions as those of the laser structure on a GaAs/Si (0 0 1) substrate. The AFM image shows good QD uniformity and dot density of ~4×10^{10} cm^{-2}. Room temperature PL was employed to measure the optical properties of InAs/GaAs QDs. A comparison of PL results for InAs/GaAs QDs grown on GaAs/Si (0 0 1) and native GaAs substrates under the same growth conditions is shown in Fig. 2(c). Here, ground state (GS) PL emission of InAs/GaAs QDs grown on GaAs/Si (0 0 1) and GaAs substrates at ~1308 nm and 1314 nm, respectively, is observed. The PL emission of the InAs/GaAs QDs on GaAs/Si (0 0 1) shows a slight blue shift to that of InAs/GaAs QDs on GaAs, which is caused by residual strain. The full-width at half-maximum (FWHM) for both samples is ~32 meV. The PL peak intensity of InAs/GaAs QDs on GaAs/Si (0 0 1) is about ~85% of that of QDs on native GaAs substrate. The lower PL peak intensity of GaAs/Si (0 0 1) based QDs may have been caused by relatively higher number of TDs in the active region that can act as non-radiative centers. Fig. 2(d) shows a cross-sectional TEM image of a typical QD in well structure which was grown in a 2 nm $In_{0.16}Ga_{0.84}As$ well and capped with a 6.5 nm $In_{0.16}Ga_{0.84}As$ capping layer. As shown in Fig. 2(d), typical dot dimensions of ~11.3 nm height and ~24.4 nm in diameter were obtained.

Measurements of temperature dependent PL have been used for studying the optical properties of InAs/GaAs QDs directly grown on a GaAs/Si (0 0 1) substrate. Fig. 3(a) displays temperature-dependent PL spectra from 20 K to 300 K. Fig. 3(b) shows the temperature dependence of PL intensity and FWHM for both excited state (ES) and GS. This reveals that the intensities of all emission states decrease with increasing temperature, and that the GS intensities show much sharper slope as unsaturated GS is more sensitive to non-radiative recombination enhanced by increasing temperature [34]. The FWHM for GS emission remain relatively constant, which indicates good QD uniformity. However, some fluctuation is observed for ES between 100 K and 200 K. This can be attributed to the thermal energy having influence on the carrier population of GS, leading to saturation at certain temperatures, and hence, broadening of the ES linewidth. A common cause of spectrum broadening at low temperatures is additional emission from small QDs. In contrast, at high temperatures, dominant QDs

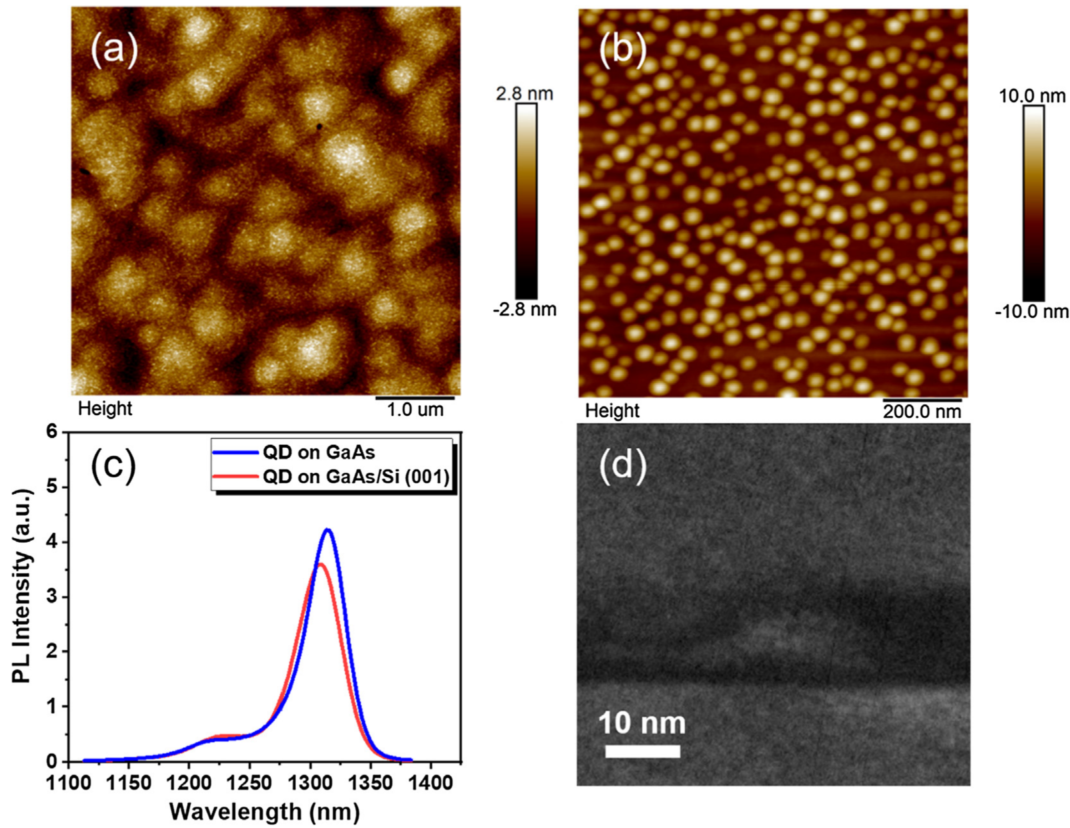

Fig. 2. (a) A 5 µm × 5 µm AFM image of a 400 nm GaAs buffer directly grown on on-axis Si (0 0 1) substrate. (b) A 1 µm × 1 µm AFM image of uncapped QDs grown on GaAs/Si (0 0 1) substrate. (c) A comparison of PL results for InAs/GaAs QDs grown on GaAs/Si (0 0 1) and native GaAs substrate at same condition. (d) A cross-sectional TEM image of a typical InAs/GaAs QD.

with high localization energy are more easily occupied by carriers [35].

Fig. 4(a) shows a cross-sectional 220 bright-field TEM image of the III-As buffer including a GaAs buffer layer and four sets of DFLs. TDD clearly decreases from bottom to top of the buffer structure. A reduced number of TDs is observed after passing each repeat of SLSs. Reactions between TDs and changes in the dislocation direction, forming misfit segments are the maim mechanisms to reduce the dislocation density [36]. Significant reduction in the number of TDs in the last 300 nm N-type GaAs layer is observed after the final $In_{0.18}Ga_{0.82}As/GaAs$ SLSs, indicating successful optimisation of buffer design. Total thickness of the buffer layer marked in Fig. 4(a) is ~2 µm, which could help reduce the impact of different thermal expansion coefficients of different materials, and hence, reduce the density of thermal cracks. Fig. 4(b) presents a dark field cross-sectional TEM image under (0 0 2) giving an overview of active region. Five layers of DWELL structures are coherently grown. It clearly shows that InAs/GaAs QDs are not vertically aligned due to the spacing layers grown at high temperature [37]. The visual absence of TDs in Fig. 4(b) could further prove that, following the four sets of DFLs, only minor TDs appear in the active region.

2.3. Device results and discussion

Standard photolithography and wet etching techniques were used to fabricate exact Si (0 0 1)-based InAs/GaAs QD laser material into broad-area lasers with a 50 µm strip width. A schematic diagram of the fabricated InAs/GaAs QD laser on exact (0 0 1) GaAs/Si platform is shown

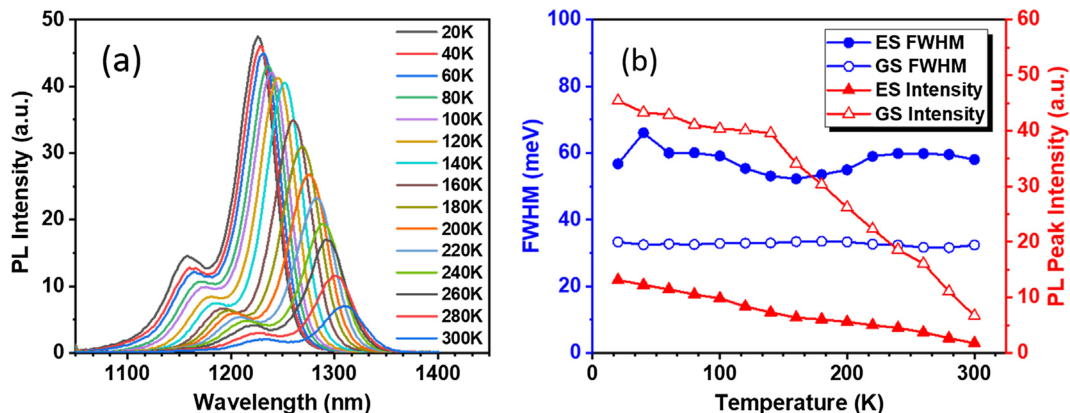

Fig. 3. (a) Temperature dependent PL spectra of InAs/GaAs QDs directly grown on GaAs/Si (0 0 1) substrate. (b) PL peak Intensity and FWHM change of ES and GS emission versus temperature from 20 K to 300 K.

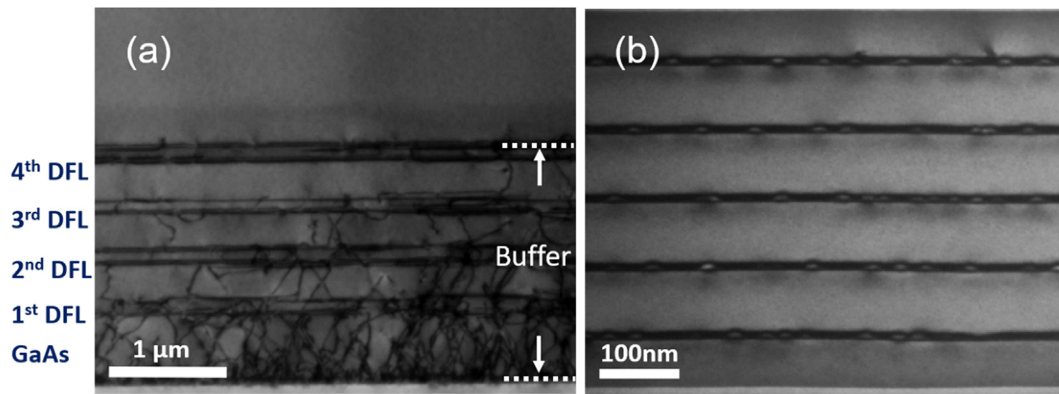

Fig. 4. (a) Cross-sectional TEM image for whole buffer including DFLs. (b) Cross-section TEM image for active region with InAs/GaAs DWELL structure.

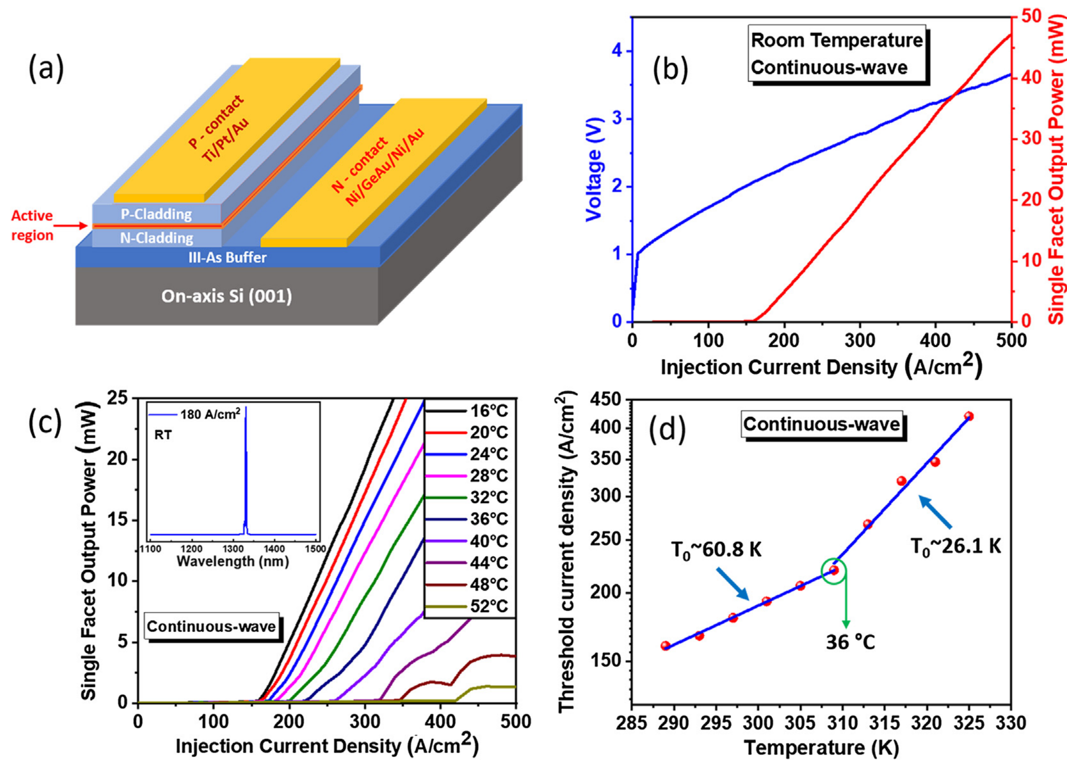

Fig. 5. (a) Schematic diagram of fabricated InAs/GaAs QD laser on GaAs/Si (0 0 1). (b) LIV characteristic of 50 µm × 3 mm broad-area InAs/GaAs QD laser directly grown on GaAs/Si (0 0 1) substrate. (c) LI characteristics of InAs/GaAs QD laser directly grown on GaAs/Si (0 0 1) at various operation temperature. The inset shows a lasing spectrum at 180 A/cm^2 injection current density. (d) Temperature dependence of threshold current density for InAs/GaAs QD laser directly grown on GaAs/Si (0 0 1) substrate from 16 °C to 52 °C.

in Fig. 5(a). The last 300 nm highly doped N-type GaAs layer in DFL below $Al_{0.4}Ga_{0.6}As$ cladding layer was etched for N-type contact (Ni/GeAu/Ni/Au) deposition by thermal evaporation. The top P-type GaAs contact layer was etched down about 200 nm and Ti/Pt/Au layer was deposited by sputtering to form a P-type metal contact. After thinning the Si substrate down to 120 µm, laser bars were cleaved into 3 mm cavity length without applying facet coating. The completed devices were mounted on copper heatsinks and bonded with gold wires for further lasing characteristic measurements.

Fig. 5(b) presents a light-current-voltage (LIV) characteristic for the broad-area InAs/GaAs QD laser on GaAs/Si (0 0 1). The light-current (LI) curve shows a low J_{th} of ~160 A/cm^2 at room temperature under CW operation mode, which is a significant improvement compared to our previously reported results on GaAs/Si (0 0 1) [26]. Moreover, as the device has been fabricated by As-only growth and has a buffer as thin as ~2 µm, the compatibility of the device with industry standard fabrication process has also improved. Furthermore, for the LI curve, a single facet output power of 48 mW is obtained at injection current density of 500 A/cm^2 with no thermal rollover. The calculated slope efficiency and external differential quantum efficiency achieved are ~0.095 W/A and 9.95%, respectively, which indicate an improvement to our previous results (~0.068 W/A and 7.20%) [26]. As heating affects the laser performance under CW mode, improved slope efficiency leads to a better temperature stability of device. To have a quantitative investigation, the temperature dependence of J_{th} and characteristic temperature T_0 are shown in Fig. 5(c) and (d).

Fig. 5(c) presents the LI characteristics of InAs/GaAs QD laser on GaAs/Si (0 0 1) at various operation temperatures under CW mode. The J_{th} increases with the rising of operation temperature, and lasing was observed up to 52 °C. Also, the LI characteristic at 52 °C shows thermal rollover of the output power which can be due to the self-heating of the device. Hard soldering to high thermal conductivity heatsinks may help

to improve the temperature performance of device. The inset in Fig. 5(c) presents a laser emission spectrum with injection current density of 180 A/cm^2 at room temperature, which shows the lasing wavelength at O-band. Temperature-dependence of J_{th} is shown in Fig. 5(d). The calculated characteristic temperature T_0 of ∼60.8 K was between 16 °C and 36 °C under CW mode. At higher temperatures 36–52 °C, the characteristic temperature T_0 was degraded to ∼26.1 K. For the next step, the characteristic temperature T_0 could be further improved by introducing P-type modulation doping technique.

3. Conclusion

In conclusion, we have successfully demonstrated an electrically pumped CW 1.3 µm InAs/GaAs QD laser directly grown on CMOS-compatible Si (0 0 1) substrate operating at maximum temperature of 52 °C with a reduced thickness of ∼2 µm high quality III-As buffer layer, including $In_{0.18}Ga_{0.82}As$/GaAs DFLs. A low J_{th} down to 160 A/cm^2 is achieved. A single facet output power of 48 mW was observed without thermal rollover at 500 A/cm^2. Much higher output power can be expected with higher injection current density. Lasing was observed up to 52 °C with a calculated characteristic temperature T_0 of 60.8 K from 16 °C to 36 °C under CW operation mode. Further improvement in the temperature characteristics on this platform is possible with improved fabrication process. Monolithically integrated InAs/GaAs QD lasers on exact Si (0 0 1), without intermediate buffer, provide a promising approach for implementing high-performance, CMOS-compatible and low-cost on-chip light sources for Si photonics, which can be seen as a major step towards its commercialization.

Acknowledgement

The authors acknowledge financial support from UK EPSRC under, Grant No EP/P006973/1, and EPSRC National Epitaxy Facility. European project H2020-ICT-PICTURE (780930); Royal Academy of Engineering (RF201617/16/28). Investissments d'avenir (IRT Nanoelec: ANR-10-IRT-05 and Need for IoT: ANR-15-IDEX-02). S.C. thanks the Royal Academy of Engineering for funding his Research Fellowship.

References

[1] M. Asghari, A.V. Krishnamoorthy, Silicon photonics: energy-efficient communication, Nat. Photon. 5 (2011) 268–270.
[2] A. Rickman, The commercialization of silicon photonics, Nat. Photon. 8 (8) (2014) 579–582.
[3] Z. Zhou, B. Yin, J. Michel, On-chip light sources for silicon photonics, Light Sci. Appl. 4 (11) (2015) 1–13.
[4] D. Liang, J.E. Bowers, Recent progress in lasers on silicon, Nat. Photon. 4 (8) (2010) 511–517.
[5] Z. Wang, B. Tian, M. Pantouvaki, W. Guo, P. Absil, J. Van Campenhout, C. Merckling, D. Van Thourhout, Room-temperature InP distributed feedback laser array directly grown on silicon, Nat. Photon. 9 (12) (2015) 837–842.
[6] H. Rong, A. Liu, R. Jones, O. Cohen, D. Hak, R. Nicolaescu, A. Fang, M. Paniccla, An all-silicon Raman laser, Nature 433 (7023) (2005) 292–294.
[7] R.E. Camacho-Aguilera, Y. Cai, N. Patel, J.T. Bessette, M. Romagnoli, L.C. Kimerling, J. Michel, An electrically pumped germanium laser, Opt. Express 20 (10) (2012) 11316.
[8] J. Liu, X. Sun, D. Pan, X. Wang, L.C. Kimerling, T.L. Koch, J. Michel, Tensile-strained, n-type Ge as a gain medium for monolithic laser integration on Si, Opt. Express 15 (18) (2007) 11272.
[9] Y. Arakawa, H. Sakaki, Multidimensional quantum well laser and temperature dependence of its threshold current, Appl. Phys. Lett. 40 (11) (1982) 939–941.
[10] S.M. Chen, M.C. Tang, J. Wu, Q. Jiang, V.G. Dorogan, M. Benamara, Y.I. Mazur, G.J. Salamo, A.J. Seeds, H. Liu, 1.3 µm InAs/GaAs quantum-dot laser monolithically grown on Si substrates operating over 100°C, Electron. Lett. 50 (20) (2014) 1467–1468.
[11] A.Y. Liu, J. Bowers, Photonic integration with epitaxial III-V on silicon, IEEE J. Sel. Top. Quantum Electron. 24 (6) (2018) 1–12.
[12] H.-H. Chang, A.W. Fang, M.N. Sysak, H. Park, R. Jones, O. Cohen, O. Raday, M.J. Paniccia, J.E. Bowers, 1310 nm Silicon evanescent laser, Opt. Express 15 (18) (2007) 11466.
[13] K. Tanabe, K. Watanabe, Y. Arakawa, III-V/Si hybrid photonic devices by direct fusion bonding, Sci. Rep. 2 (2012) 1–6.
[14] Z. Wang, K. Van Gasse, V. Moskalenko, S. Latkowski, E. Bente, B. Kuyken, G. Roelkens, A III-V-on-Si ultra-dense comb laser, Light Sci. Appl. 6 (5) (2017) e16260.
[15] E. Tournié, L. Cerutti, J.-B. Rodriguez, H. Liu, J. Wu, S. Chen, Metamorphic III–V semiconductor lasers grown on silicon, MRS Bull. 41 (03) (2016) 218–223.
[16] J. Wu, S. Chen, A. Seeds, H. Liu, Quantum dot optoelectronic devices: lasers, photodetectors and solar cells, J. Phys. D. Appl. Phys. 48(36) (2015).
[17] R. Beanland, A.M. Sánchez, D. Childs, K.M. Groom, H.Y. Liu, D.J. Mowbray, M. Hopkinson, Structural analysis of life tested 1.3 µm quantum dot lasers, J. Appl. Phys. 103 (1) (2008) 2–7.
[18] M. Tang, S. Chen, J. Wu, Q. Jiang, V.G. Dorogan, M. Benamara, Y.I. Mazur, G.J. Salamo, A. Seeds, H. Liu, 1.3 µm InAs/GaAs quantum-dot lasers monolithically grown on Si substrates using InAlAs/GaAs dislocation filter layers, Opt. Express 22 (10) (2014) 11528–11535.
[19] V.K. Yang, M. Groenert, C.W. Leitz, A.J. Pitera, M.T. Currie, E.A. Fitzgerald, Crack formation in GaAs heteroepitaxial films on Si and SiGe virtual substrates, J. Appl. Phys. 93 (7) (2003) 3859–3865.
[20] T. Wang, H. Liu, A. Lee, F. Pozzi, A. Seeds, 1.3 µm InAs/GaAs quantum-dot lasers monolithically grown on Si substrates, Opt. Express 19 (12) (2011) 11381–11386.
[21] A. Lee, Q. Jiang, M. Tang, A. Seeds, H. Liu, Continuous-wave InAs/GaAs quantum-dot laser diodes monolithically grown on Si substrate with low threshold current densities, Opt. Express 20 (20) (2012) 22181.
[22] M. Liao, S. Chen, S. Chen, S. Huo, J. Wu, M. Tang, K. Kennedy, W. Li, S. Kumar, M. Martin, T. Baron, C. Jin, I. Ross, A. Seeds, H. Liu, Monolithically integrated electrically pumped continuous-wave III-V quantum dot light sources on silicon, IEEE J. Sel. Top. Quantum Electron. 23 (6) (2017).
[23] Y. Wang, S. Chen, Y. Yu, L. Zhou, L. Liu, C. Yang, M. Liao, M. Tang, Z. Liu, J. Wu, W. Li, I. Ross, A.J. Seeds, H. Liu, S. Yu, Monolithic quantum-dot distributed feedback laser array on silicon, Optica 5 (5) (2018) 528–533.
[24] M. Liao, S. Chen, Z. Liu, Y. Wang, L. Ponnampalam, Z. Zhou, J. Wu, M. Tang, S. Shutts, Z. Liu, P.M. Smowton, S. Yu, A. Seeds, H. Liu, Low-noise 1.3 µm InAs/GaAs quantum dot laser monolithically grown on silicon, Photon. Res. 6 (11) (2018) 1062.
[25] S. Chen, W. Li, J. Wu, Q. Jiang, M. Tang, S. Shutts, S.N. Elliott, A. Sobiesierski, A.J. Seeds, I. Ross, P.M. Smowton, H. Liu, Electrically pumped continuous-wave III–V quantum dot lasers on silicon, Nat. Photon. 10 (5) (2016) 307–311.
[26] S. Chen, M. Liao, M. Tang, J. Wu, M. Martin, T. Baron, A. Seeds, H. Liu, Electrically pumped continuous-wave 1.3 µm InAs/GaAs quantum dot lasers monolithically grown on on-axis Si (001) substrates, Opt. Express 25 (5) (2017) 4632–4639.
[27] J. Norman, M.J. Kennedy, J. Selvidge, Q. Li, Y. Wan, A.Y. Liu, P.G. Callahan, M.P. Echlin, T.M. Pollock, K.M. Lau, A.C. Gossard, J.E. Bowers, Electrically pumped continuous wave quantum dot lasers epitaxially grown on patterned, on-axis (001) Si, Opt. Express 25 (4) (2017) 3927.
[28] K. Volz, A. Beyer, W. Witte, J. Ohlmann, I. Nmeth, B. Kunert, W. Stolz, GaP-nucleation on exact Si (001) substrates for III/V device integration, J. Cryst. Growth 315 (1) (2011) 37–47.
[29] A.Y. Liu, J. Peters, X. Huang, D. Jung, J. Norman, M.L. Lee, A.C. Gossard, J.E. Bowers, Electrically pumped continuous-wave 1.3 µm quantum-dot lasers epitaxially grown on on-axis (001) GaP/Si, Opt. Lett. 42 (2) (2017) 338–341.
[30] D. Jung, Z. Zhang, J. Norman, R. Herrick, M.J. Kennedy, P. Patel, K. Turnlund, C. Jan, Y. Wan, A.C. Gossard, J.E. Bowers, Highly reliable low-threshold InAs quantum dot lasers on on-axis (001) Si with 87% injection efficiency, ACS Photon. 5 (3) (2018) 1094–1100.
[31] J. Kwoen, B. Jang, J. Lee, T. Kageyama, K. Watanabe, Y. Arakawa, All MBE grown InAs/GaAs quantum dot lasers on on-axis Si (001), Opt. Express 26 (9) (2018) 11568.
[32] R. Alcotte, M. Martin, J. Moeyaert, R. Cipro, S. David, F. Bassani, F. Ducroquet, Y. Bogumilowicz, E. Sanchez, Z. Ye, X. Bao, J. Pin, T. Baron, Epitaxial growth of antiphase boundary free GaAs layer on 300 mm Si (001) substrate by metalorganic chemical vapour deposition with high mobility, APL Mater. 4 (4) (2016) 046101.
[33] M. Tang, S. Member, S. Chen, J. Wu, Q. Jiang, K. Kennedy, P. Jurczak, M. Liao, S. Member, R. Beanland, A. Seeds, H. Liu, A. Iii, Optimizations of defect filter layers for 1.3 µm InAs/GaAs quantum-dot lasers monolithically grown on Si substrates, IEEE J. Sel. Top. Quantum Electron. 22 (6) (2016).
[34] A.A. Bdollahinia, S.B. Anyoudeh, A.R. Ippien, F.S. Chnabel, E. Yal, I.C. Estier, I.K. Alifa, E.M. Entovich, G.E. Isenstein, R. Eithmaier, Temperature stability of static and dynamic properties of 1.55 µm quantum dot lasers, Opt. Express 26 (5) (2018).
[35] T. Wang, H.Y. Liu, J.J. Zhang, Temperature-dependent photoluminescence characteristics of InAs/GaAs quantum dots directly grown on Si substrates, Chin. Phys. Lett. 33 (4) (2016) 31–35.
[36] R. Beanland, D.J. Dunstan, P.J. Goodhew, Plastic relaxation and relaxed buffer layers for semiconductor epitaxy, Adv. Phys. 45 (2) (1996) 87–146.
[37] H.Y. Liu, I.R. Sellers, T.J. Badcock, D.J. Mowbray, M.S. Skolnick, K.M. Groom, M. Gutiérrez, M. Hopkinson, J.S. Ng, J.P.R. David, R. Beanland, Improved performance of 1.3 µm multilayer quantum-dot lasers using a high growth-temperature GaAs spacer layer, Appl. Phys. Lett. 85 (2004) 704.